Differentiable CFD and application based on Lattice Boltzmann Method

Zhuo You *, Ziqi Xu, Yicang Huang, Peng He, Hao Zhang

Wuhan Second Ship Design and Research Institute, Wuhan, China

* Corresponding Author Email: zhuoyouzju@zju.edu.cn

Abstract. For the topology optimization design problem (TO) in fluid mechanics, this paper designs a topology optimization design method based on the Lattice Boltzmann Method (LBM). The backward gradient of the flow field is obtained using differentiable algorithms, and the topology is used to optimize the topology structure. The present report selects a typical optimization problem of surface drag, including a representative problem of reduction of resistance, and verifies the algorithm. The analysis is focused on the cases of obstacles, and the results show that the present method can effectively optimize the topology structure in the flow field, with the potential to improve the design efficiency.

Keywords: Differentiable, CFD, Topology Optimization, LBM, Drag.

1. Introduction

Differentiable optimization design is the summary of a type of optimization design methods for solving engineering problems. Its fundamental principle is to establish a positive model from design parameters to predict the target parameters, while also establishing a differentiable gradient model from the target parameters to the design parameters, using the gradient descent method to directly solve the design parameters using the target parameter as the optimization subject. In the new design of vehicles, the design parameters of differentiable optimization design are generalization to a wider design scope, which can maintain scientific principles while overcome given limitations.

Currently, differentiable simulation and design methods for high-Reynolds number flow fields are still Blank. Currently available professional CFD software such as Fluent, CFX, and the emerging Power Flow in the automotive design field are still only able to perform positive simulation under the condition of known structural parameters, and cannot solve the differentiable gradient of the structural parameters. However, due to the complexity of solving the fluid control equations (i.e. the N-S equation and the Navier-Stokes equation), the TO technology belongs to the differentiable design method is although relatively mature in the mechanical structure field, yet cannot be widely adopted in fluid computing. Currently, only a few commercial software such as Comsol have modules for differentiable TO design in low-Reynolds number flow fields (such as for differentiable -structure-material).

By introducing the backpropagation method in the field of artificial intelligence, it is possible to obtain numerical expressions for the full design input of a flow field simulation model with high Reynolds number, and to achieve rapid optimization design. As shown in Figure 1, artificial intelligence mainly solves the problem of an uncertain physical model from the input x to the predict output y. Therefore, using a large number of training data through the backpropagation and gradient descent optimization methods, we fit the network model parameters that minimize the prediction loss, and then deploy them in the case of solving y(x). For differentiable simulation design of specific objects, the predict model from x to y already has a simulation physical model, such as CFD and finite element, because it does not require a large number of training data to train the model. Therefore, it can accelerate, such as flow field simulation of turbulent flow, problems that require a large number of computational resources.

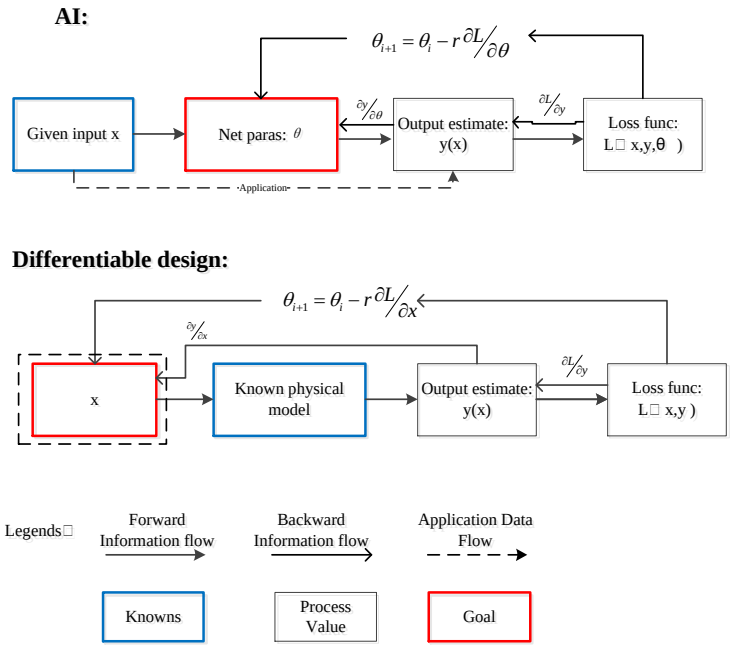

Figure 1. Differentiable design and AI model

In CFD calculations, the LBM is easier to obtain numerical expressions for the input than traditional CFD software because it does not require the finite difference method for solving the Navier-Stokes equation (NS equation), which makes it possible to solve problems with small values of the Reynolds number that are stable. The main problem with early LBM applications was that the Reynolds number that was stable was small (e.g. 1000). After improving the LBM model by Geiier et al. [1] in 2006 the CM-MRT model, (Central-Moment Multiple-Relaxation- Times Model was able to simulate flows with viscosity approaching zero. In 2021, Wei Li et al. [2] further improved the stability and accuracy of the calculation by conducting higher-dimensional expansion calculations and updated the boundary treatment method [3].

The differentiable programming language Taichi [4] has been developed as an open-source programming language in the field of computer vision in recent years. Its differentiable programming optimization computational thinking has shown great potential in terms of structural TO [5], software robots and its control [6]. It has already been applied in LBM research [7].

Therefore, in order to explore rapid and innovative design methods in the field of fluid mechanics, this paper uses the LBM method and the differentiable -programming language Taichi to investigate differentiable simulation methods for high-Reynolds number flow fields, achieving the backward differential solution of the simulation results on the fluid topology.

2. Method

2.1. Problem Definition

One of the classical examples of differentiable fluid TO (DFTO) is shown in Figure 2. The shape of the obstacle in the two-dimensional flow field is optimized to reduce its drag. The flow field region is a long and narrow rectangular, with the left side as the entrance, the right side and the upper and lower boundaries as the exit boundaries. The upper and lower boundaries are designed to use the exit boundary instead of the solid wall boundary conditions to reduce the numerical oscillations and convergence caused by the accumulation of sonic boundary reflection.

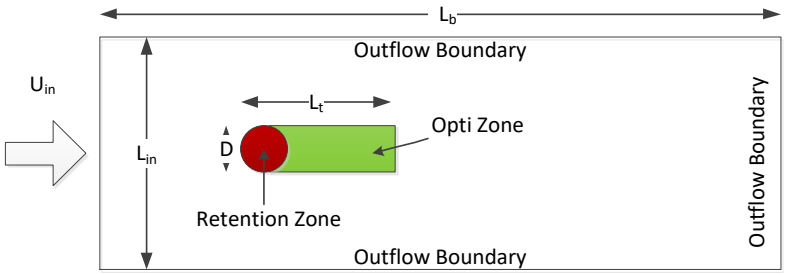

Figure 2. Definition of DFTO problem

The retention area without optimization in the obstacle is a circular area, which can be understood as the load that the optimized result needs to carry. The object optimization area is a rectangular area that is the downstream of the circular area from the entrance flow rate. After pre-flight calculations, it was found that the circular area at the center of the retention area, passing through the center of the object optimization area on the right, will be optimized as a flow area, as shown in Figure 3. Therefore, the optimization area is set in the current form.

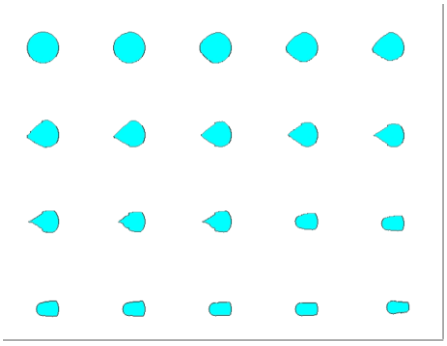

Figure 3. The gradual solution of the optimization of reducing resistance in the initial large circular area.

2.2. Calcualtion Process

The calculation of resistance is obtained by taking the integral of the force acting on all cells on the obstacle. The force calculation on the boundary is also performed during the collision process. For the cell C_b, the force on its neighbor cells C_n during the collision process is:

$$f_{(C_b,k,i+1)} = f_{C_b,k,i} + (f_{eq(C_b,k)} - f_{eq(C_n,k)}) \tag{1}$$

The statistical resistance acts on all particles with a density greater than 0.5, and the force on all particles in the direction of their movement is combined:

$$F_x = \sum_{k=0}^{8} f(C_b,k)e_{k,x} \mid \rho(C_b) > 0.5 \tag{2}$$

The mathematical representation of the optimization process is:

- ✧ Optimization function: min (F_x);
- ✧ Optimization parameter: ρ (C_b);
- ✧ Subject to: MRT-LBM equation, calculation area and boundary condition.

The process flow of the optimization calculation is shown in Figure 4. The optimization algorithm uses the density method, and during the process of calculating the flow field using the LBM method and summarize the results of the resistance on the obstacle, the differentiate state of variables from topo density to resistance are recorded. After obtaining the resistance value, the gradient value is calculated using the backpropagation method to obtain the derivative with respect to topo density. Since the value of the derivative in a single-step calculation process is small, and the state at the boundary is often stable, the derivative is cumulated by multiple steps before the update of the topo is performed. The convergence criteria are whether the calculated steps have reached the max steps.

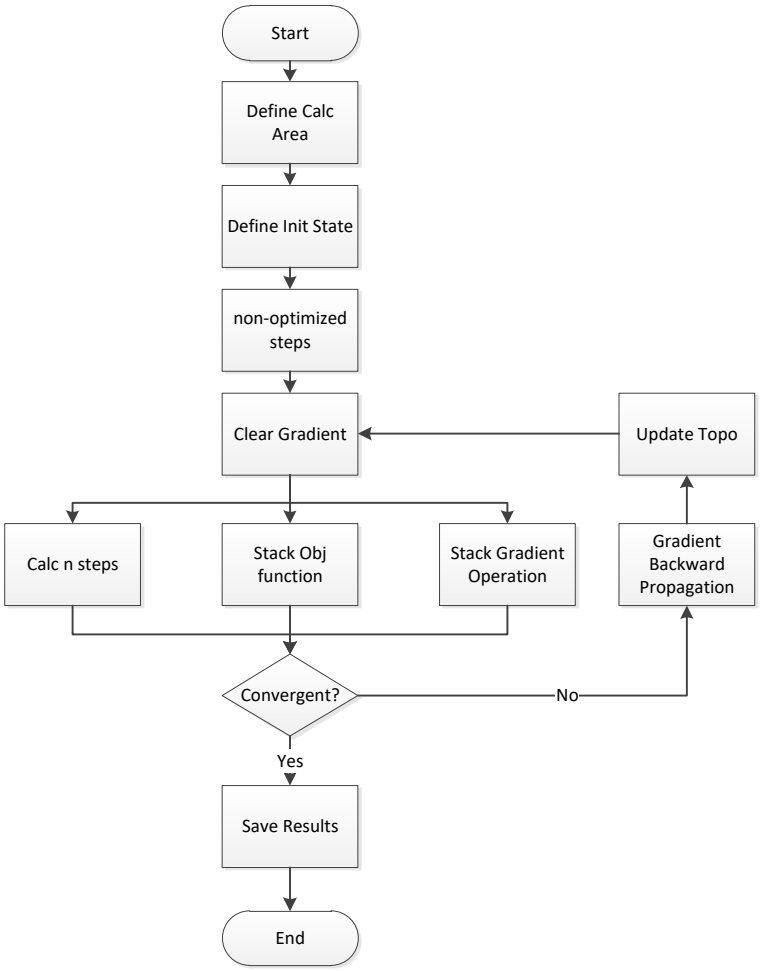

Figure 4. Process flow of the optimization calculation

2.3. Numerical Test Conditions

Calculate the optimization process through three conditions, with specific initial parameters as shown in Table 1, length units are grid units and time units are unit grids / speed of sound. The calculation region is set to be 800 long, with an inlet width of 200 and an inlet flow velocity of 0.1. The diameter of the obstacle is 20. The lengths of the optimized areas for the three conditions are respectively set to 50, 50, and 30, with dynamic viscosities set to 0.005, 0.01, and 0.01. To consider the differences between the conditions from the perspective of computational stability, the Reynolds number calculated using the calculation area length as the characteristic scale is uniformly set to 1.6×10^4. When examining the differences between the conditions, the Reynolds numbers based on the initial total length of obstacles are 1200, 600, and 400, respectively.

Table 1. Numerical Test Conditions

No.	Name	Case 1	Case 2	Case 3
	L_{in}	800		
	L_b	200		
	D	20		
	L_t	50	50	30
	U_{in}	0.1		
	v	0.005	0.01	0.01
	Re_c	1.6×10^4		
	Re_p	1.2×10^3	0.6×10^3	0.4×10^3

Optimization calculation parameter settings are as follows:

- ✧ Initial non-optimized steps: 20,000

- ✧ Gradient optimization times: 2,000
- ✧ Single optimization statistical step: 200
- ✧ Total computation steps: 4.2×10^5

3. Result and Discussion

The resistance convergence curves for three operating conditions in the optimization process are shown in Figure 5. All three curves experience a rapid decline in resistance values within the first 100 optimization steps, and then the decline becomes smaller over the subsequent 1,900+ steps. This indicates that most of the topology pruning work has been completed around the 50th optimization step, and further explanations will be provided in the next section. This demonstrates that this method can achieve efficient topological optimization design in the flow field.

All three operating conditions show small amplitude oscillations in their resistance values during the subsequent optimization calculations. This is related to the fact that the flow field itself is in an unstable turbulent oscillation state.

Figure 5 also shows that the resistance for all three operating conditions has significantly decreased after optimization, with a reduction of about 50-60%. This indicates the effectiveness of this method for drag optimization. It should be noted that this method is based on gradient descent, and the results obtained are local optima rather than global optima. Although the multi-step averaging method has been used to some extent for regional search. There is still room for improvement by introducing more advanced optimization algorithms to improve this algorithm.

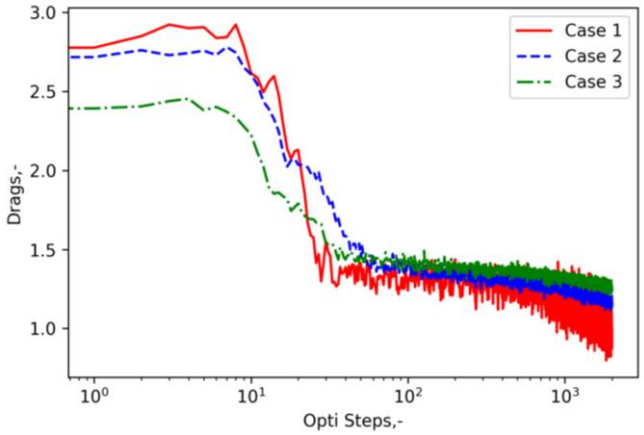

Figure 5. Drags during the optimization process for the three operating conditions

Figure 6 presents the topology optimization results for the three operating conditions. Each of the optimization results exhibits a “teardrop” shape with a rounded tail, differing from the traditional concept of a teardrop shape, where the tail is a sharp angle. The comparison with traditional teardrop shapes due to dimensions, Reynolds number, etc., is not within the scope of this discussion.

When comparing the results with respect to Case 2 as the baseline, we observe that for Case 1, increasing the Reynolds number leads to an additional horizontal rectangular segment of equal width as the head at the center; for Case 3, reducing the initial feasible optimization area by truncating the tail results in an optimization result similar to the shape obtained from Case 2 after truncation at the corresponding size, with an increased tail size.

Combining this information with the resistance values shown in Figure 5, we find that although Case 3 has a larger wet surface area and higher resistance, the optimized resistance value is comparable to that of Case 2, even slightly lower than Case 3. This indicates that the calculation region needs to be sufficiently large enough to ensure sufficient solution space for finding the optimal value.

In summary, the presented results show that the optimization calculation region should be large enough to accommodate sufficient solution space for finding the optimal value, taking into account

the differences in dimensions, Reynolds number, and other factors between the three operating conditions.

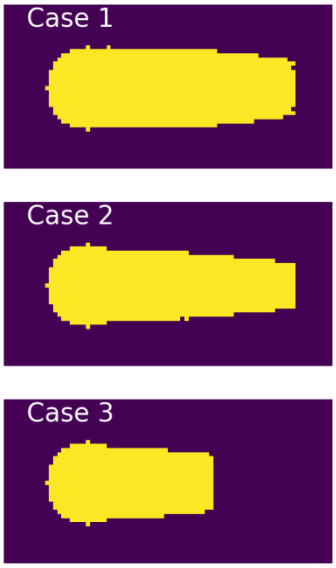

Figure 6. The topology optimization results for the three operating conditions

Figure 7 shows the topology, velocity field, and vortex field at step 50 and calculation step 30,000 during optimization for Case 2. When compared with the topology of Case 2 in Figure 6, the result in Figure 7 already has the outlines of the final calculation results, indicating that this algorithm has the potential for rapid iteration and design scheme improvements, thereby enhancing design efficiency.

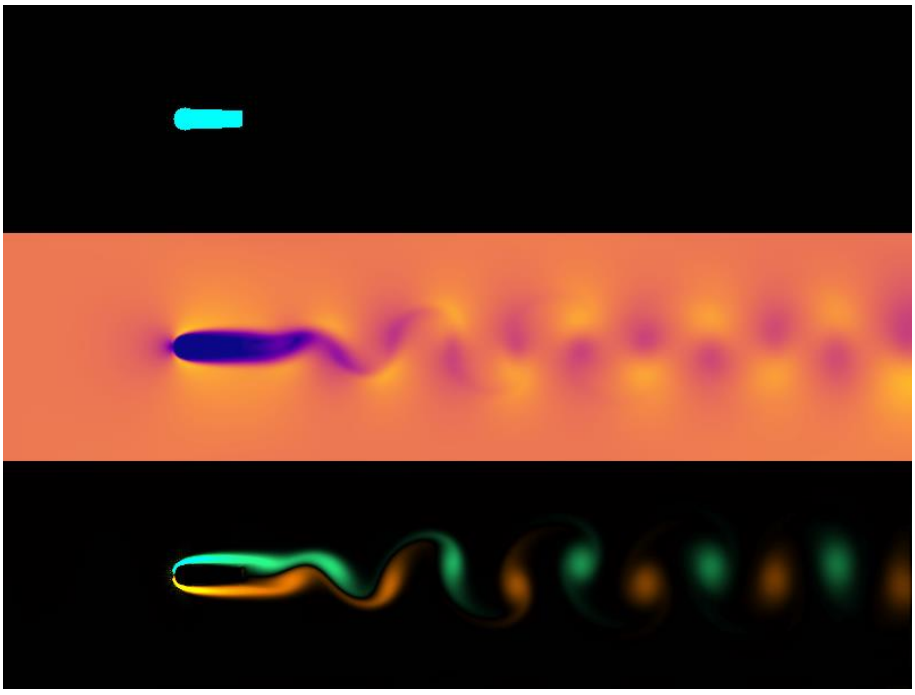

Figure 7. Case 2, Opti step: 50, calculation step:30000: topology structure (up), velocity(mid) and vortex (down)

It seems likely that the initial distribution of the computational domain in these three examples did not significantly affect the flow field structure, as both the initial and optimized results showed relatively minor differences in terms of topology forms.

4. Conclusion

This report introduces the method of topology optimization for differentiable flow fields and verifies it using an example involving optimizing for drag force around a bluff body. The following conclusions can be summarized from the three cases studied:

(1) The method presented here is capable of efficiently optimizing the topology of flow fields, which has the potential to accelerate design iterations and improve overall design efficiency.

(2) For the obstacle problem, increasing the Reynolds number after optimization leads to the formation of a horizontal rectangular segment with a diameter equal to that of the head in the middle part.

(3) In practical applications, if there is good experience and knowledge of fluid dynamics, it is recommended to adopt schemes with more reasonable initial topology conditions. Conversely, for exploratory problems, it is advisable to increase the solution space reasonably to enhance the possibility of discovering innovative solutions.

The feasibility and potential of the differentiable optimization algorithm have been demonstrated in this report; however, there are numerous areas for improvement in practice, such as improving stability at high Reynolds numbers, advancing to 3D dimensions, enhancing accuracy for irregular boundary calculations, adopting unstructured grids, applying more advanced optimization methods, and incorporating fluid-solid coupling and multiphase flows.

Acknowledgements

The authors would like to express their heartfelt gratitude to Wang [7] for his work in programming LBM using Taichi language, elegant result presentation, and open sharing.

References

[1] Martin Geier, Andreas Greiner and Jan G. Korvink. Cascaded digital lattice Boltzmann automata for high Reynolds number flow. Physical Review E73, 066705(2006).

[2] ChaoYang Lyu, Wei Li, Mathieu Desbrun, et al. Fast and Versatile Fluid-Solid Coupling for Turbulent Flow Simulation, ACM Trans. Graph, Vol. 40, No.6, Article 201, 2021.

[3] Wei Li, Yixin Chen, Mathieu Desbrun. Fast and Scalable Turbulent Flow Simulation with Two-Way Coupling. ACM Trans. Graph., Vol. 39, No. 4, Article 1. July 2020.

[4] Hu, Y., T. Li, L. Anderson, J. Ragankelley and F. Durand (2019). Taichi: A Language for High-Performance Computation on Spatially Sparse Data Structures. ACM Transactions on Graphics 38(6): 1-16.

[5] Liu, H., Y. Hu, B. Zhu, W. Matusik and E. Sifakis. Narrow-band topology optimization on a sparsely populated grid. ACM Transactions on Graphics 37(6): 1-14. 2018.

[6] Hu, Y., L. Anderson, T. Li, Q. Sun, N. A. Carr, J. Ragankelley and F. Durand (). DiffTaichi: Differentiable Programming for Physical Simulation: 1-20, 2020.

[7] Wang, https://raw.githubusercontent.com/hietwll/, 2020.